Visible-blind, ultraviolet-sensitive photodetector based on $SrTiO_3$ single crystal

J. Xing,[1] K. Zhao,[2] H. B. Lu,[1,*] X. Wang,[1] G. Z. Liu,[1] K. J. Jin,[1] M. He,[1] C. C. Wang,[1] and G. Z. Yang[1]

[1]*Beijing National Laboratory for Condensed Matter Physics, Institute of Physics, Chinese Academy of Sciences, Beijing 100080, China*

[2]*Department of Mathematics and Physics, China University of Petroleum, Beijing 102249, China*

[*]*Corresponding author: hblu@aphy.iphy.ac.cn*

Received May 23, 2007; revised July 17, 2007; accepted July 30, 2007;
posted July 31, 2007 (Doc. ID 83377); published August 17, 2007

High-sensitivity and visible-blind ultraviolet (UV) photoconductive detectors based on $SrTiO_3$ single crystal with interdigitated electrodes are reported. The responsivities of photovoltage and photocurrent can reach 2.13×10^5 V/W and 213 mA/W, respectively, at 330 nm at ambient temperature, and the corresponding quantum efficiency η reaches 80.2%. The dark current is lower than 50 pA at 10 V bias, and the UV/visible contrast ratio is about four orders of magnitude with a sharp cutoff at 390 nm. The experimental results demonstrate that $SrTiO_3$ single crystal has potentially wide applications in UV detection. © 2007 Optical Society of America

OCIS codes: 040.5160, 040.7190, 260.5150.

Perovskite-type metal oxides, which could be expected to exhibit novel characteristics and display high sensitivity to external magnetic and electric fields, have attracted considerable attention [1–4]. One of the important characteristics of perovskite materials is the photoelectric effect [5–7]. Ultraviolet (UV) radiation detectors have drawn a great deal of interest in recent years due to many civil and military requirements. In particular, UV detection with high discrimination against visible and infrared light is ideal for detection in the background of infrared and visible radiation. Classical semiconductors including silicon and gallium arsenide can be used in UV detection, but their long wavelength response needs to be excluded with filters. In addition, they exhibit poor radiation hardness and have high dark currents with increasing bias owing to their narrow bandgap [8]. The wide bandgap materials, such as III–V nitrides, silicon carbide, zinc oxide, and diamond, are attractive candidates for UV detectors [9–12]. Their stable physical properties and intrinsic visible blindness have motivated extensive research by many groups. However, the UV detectors based on these materials require a complicated fabrication process and high-cost manufacture.

$SrTiO_3$ (STO), one of the perovskite oxide materials, is an insulator with a bandgap of ~3.2 eV that has been used in dynamic random access memories, high-density capacitors, and electro-optic devices. The photoconductivity of STO single crystals has been studied by several groups [13–16]. We also reported on the UV photoelectric effects in $SrTiO_{3-\delta}$/Si heterojunction and tilted-orientation STO single crystals [6,7], since STO absorbs light with less than 390 nm wavelength and presents high transparency in the range of visible and infrared wavelength. In this Letter, we focus on the high responsivity in the UV region of STO single crystal photodetectors with a sharp cutoff at 390 nm at room temperature.

As-supplied STO (001) single crystal wafers with purity of 99.99% are mirror double polished in the present study. The geometries of the STO wafers we used are 5 mm × 10 mm with thickness of 0.5 mm. To obtain high responsivity, as shown in the top inset of Fig. 1, we fabricated Au interdigitated electrodes on one surface of STO wafers. Au film with 200 nm thickness was deposited onto the STO substrates by electron-gun evaporation, and standard lithography and etching were performed to define the interdigitated contact pattern. The finger width w of the interdigitated electrode is equal to its separated spacing s. The range of w and s is from 500 to 10 μm for different detectors. Due to the shadowing effect of electrodes, the irradiated active (exposed) area is 15 mm^2. The schematic circuit of measurement is shown in the bottom inset of Fig. 1. A tunable DC voltage source was taken as the bias supply V_b, and the STO detector is in series with a sampling resistance R. A 500 MHz digital oscilloscope was used to record the voltage signal across R.

Figure 1 exemplifies the steady-state photoelectric response of a STO detector with finger width of 10 μm. The photovoltaic signal V_P was recorded by

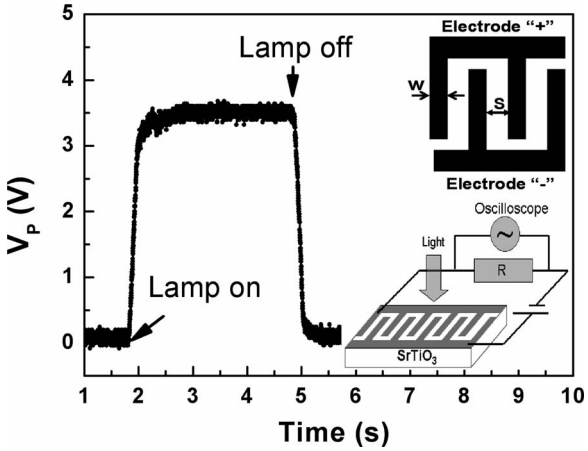

Fig. 1. Steady UV response of STO detector with $w=s=10$ μm under irradiation with an Hg lamp at a bias of 4 V. The top and bottom insets show the schematic diagrams of the interdigitated electrode configuration and the measurement system, respectively.

the oscilloscope with $R=1$ MΩ when the detector was irradiated by a monochromatic Hg lamp (253.65 nm). As shown in Fig. 1, the photovoltage was high (low) when the Hg lamp was on (off), and the voltage reached 3.5 V when the bias V_b was 4 V. The mechanism of the photovoltage is easy to understand. STO absorbed the photons and produced electron–hole pairs when STO surface was irradiated because the photon energy of 253.65 nm is higher than the bandgap of STO. Then, the light-induced electron–hole pairs were separated by the electric field of the applied bias and formed the photovoltage. So the detectors based on STO single crystal are photoconductive detectors.

Figure 2(a) shows the photocurrent I_P as a function of applied bias under steady Hg lamp irradiation with power density of 0.53 mW/cm^2. Here I_P is defined as V_P/R. The photocurrent increased linearly with the bias and did not show any trace of saturation for all detectors with different finger width. In addition, after carefully fitting the data we get $V_P \propto w^{-2}$ [solid curves in Fig. 2(b)]. These results are in agreement with the reports of photoconductive detectors [8,17].

Figure 3 shows the response with optical power density for a STO detector with 10 μm finger width at 10 V bias under the Hg lamp irradiation. From the power density of incident light, we can obtain a photocurrent responsivity of 103 mA/W and a photovoltage responsivity of 1.03×10^5 V/W. Here, we paid attention to only the exposed area (active area) and did not consider the light incident on the electrodes. The quantum efficiency η is 50%, according to the formula $\eta=R_i h\nu/q$, where h is the Planck constant, ν is the frequency of light, and q is the charge of one electron.

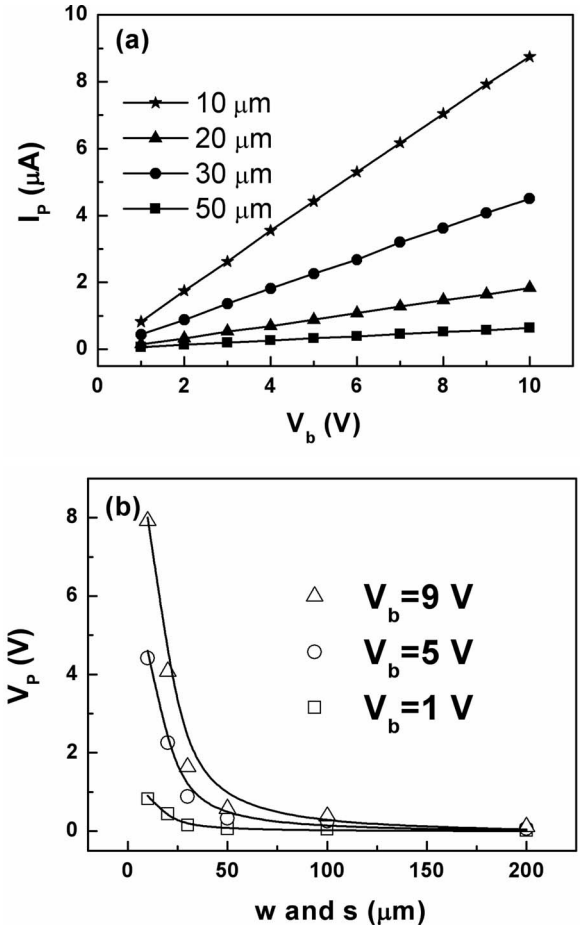

Fig. 2. (a) Bias dependence of the photocurrent for different electrode geometries. (b) Variation of photovoltage as a function of the width of finger and spacing for different biases.

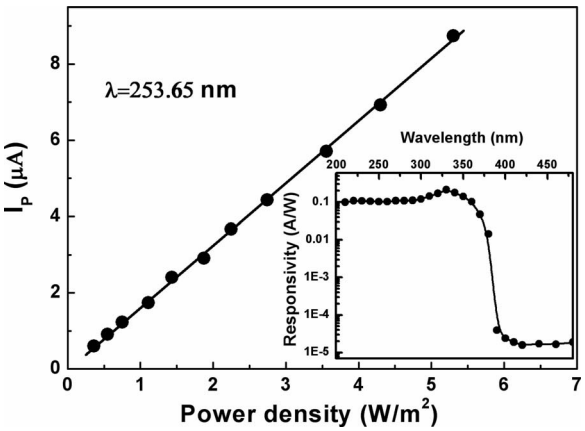

Fig. 3. Photocurrent variation with the optical power density and the spectral response (inset) of the STO detector with 10 μm finger width at 10 V bias.

The spectral responsivity was measured by a monochromator with a calibrated 75 W xenon lamp. The inset of Fig. 3 displays the spectral response of the STO detector with 10 μm finger width at 10 V bias. The wavelength of the peak response is at 330 nm, and the responsivities of photovoltage and photocurrent are 2.13×10^5 V/W and 213 mA/W, respectively. The corresponding quantum efficiency η is 80.2%, which is comparable with or even better than that of the UV detectors based on semiconductors [18–21]. From Fig. 3, we can see that the cutoff wavelength at 390 nm is very sharp, which is in agreement with the absorption spectrum [6]. The UV/visible rejection ratio is larger than 10^4, indicating that the STO detector has the property of high visible blindness. We have also measured the dark current by using a Keithley Model 2182 nanovoltmeter, and the dark current is lower than 50 pA at 10 V bias for all devices.

In addition, the third harmonic of an actively passively mode-locked Nd:YAG laser, operating at a wavelength of 355 nm with 25 ps duration, was used to measure the temporal response of the devices. Figure 4 shows a typical transient photovoltage of a STO detector with 20 μm finger and spacing at 10 V bias with a sampling resistance of $R=1$ Ω. High-speed characterization of the detector was obtained. The detector had a rise time of ~1.3 ns and a full width at half-maximum of ~1.5 ns. The slight oscillation behavior might come from impedance mismatch in the measurement circuit.

In conclusion, we have fabricated highly sensitive and visible-blind UV photodetectors based on STO single crystal with interdigitated electrodes. The cutoff wavelength at 390 nm is very sharp, with the UV/

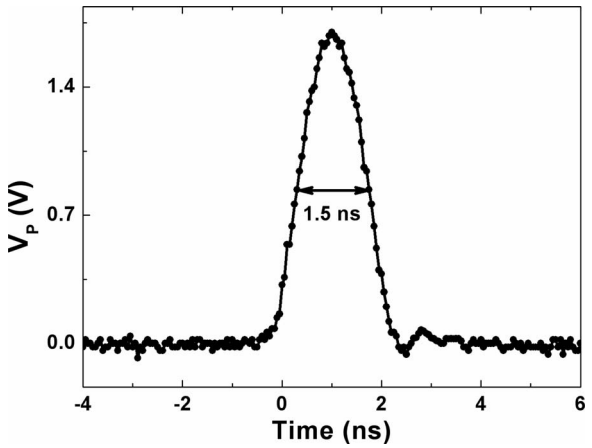

Fig. 4. Transient photovoltage of the STO detector with 20 μm finger width at 10 V bias under irradiation with a 25 ps laser pulse.

visible contrast ratio reaching four orders of magnitude. The peak response was located at 330 nm with photocurrent responsivity 213 mA/W, and the corresponding quantum efficiency η reached 80.2%. The dark current was lower than 50 pA at 10 V bias for all the devices. The present UV detectors are based on commercial STO single crystal and do not need a complicated fabrication technique or process. All of these excellent qualities demonstrate that STO single crystal is an attractive candidate for a UV detector. Further improvements of the responsivity and quantum efficiency, such as decreasing the finger width and substitution of highly transparent electrodes for Au electrodes, are ongoing.

This work is supported by the National Natural Science Foundation of China, the National Basic Research Programme of China, and the Key Project of Chinese Ministry of Education.

References

1. S. Jin, T. H. Tiefel, M. McCormack, R. A. Fastnacht, R. Ramesh, and L. H. Chen, Science **264**, 413 (1994).
2. D. Roy and S. B. Krupanidhi, Appl. Phys. Lett. **61**, 2057 (1992).
3. K.-J. Jin, H.-B. Lu, Q.-L. Zhou, K. Zhao, B.-L. Cheng, Z.-H. Chen, Y.-L. Zhou, and G.-Z. Yang, Phys. Rev. B **71**, 184428 (2005).
4. H. B. Lu, S. Y. Dai, Z. H. Chen, Y. L. Zhou, B. L. Cheng, K. J. Jin, L. F. Liu, G. Z. Yang, and X. L. Ma, Appl. Phys. Lett. **86**, 032502 (2005).
5. H. B. Lu, K. J. Jin, Y. H. Huang, M. He, K. Zhao, B. L. Cheng, Z. H. Chen, Y. L. Zhou, S. Y. Dai, and G. Z. Yang, Appl. Phys. Lett. **86**, 241915 (2005).
6. K. Zhao, K. J. Jin, Y. H. Huang, S. Q. Zhao, H. B. Hui, M. He, Z. H. Chen, Y. L. Zhou, and G. Z. Yang, Appl. Phys. Lett. **89**, 173507 (2006).
7. K. Zhao, Y. H. Huang, Q. L. Zhou, K. J. Jin, H. B. Lu, M. He, B. L. Cheng, Y. L. Zhou, Z. H. Chen, and G. Z. Yang, Appl. Phys. Lett. **86**, 221917 (2005).
8. M. Razeghi and A. Rogalski, J. Appl. Phys. **79**, 7433 (1996).
9. M. Mikulics, M. Marso, P. Javorka, P. Kordos, H. Luth, M. Kocan, A. Rizzi, S. Wu, and R. Sobolewski, Appl. Phys. Lett. **86**, 211110 (2005).
10. G. Cesare, F. Irrera, F. Palma, M. Tucci, E. Jannitti, G. Naletto, and P. Nicolosi, Appl. Phys. Lett. **67**, 335 (1995).
11. I.-S. Jeong, J. H. Kim, and S. Im, Appl. Phys. Lett. **83**, 2946 (2003).
12. A. Balducci, M. Marinelli, E. Milani, M. E. Morgada, A. Tucciarone, and G. Verona-Rinati, Appl. Phys. Lett. **86**, 193509 (2005).
13. H. Yasunaga and I. Nakada, J. Phys. Soc. Jpn. **22**, 338 (1967).
14. H. Yasunaga, J. Phys. Soc. Jpn. **24**, 1035 (1968).
15. J. W. Yoon and M. Miyayama, Jpn. J. Appl. Phys. **38**, 894 (1999).
16. H. Katsu, H. Tanaka, and T. Kawai, Jpn. J. Appl. Phys. **39**, 2657 (2000).
17. T. Palacios, E. Monroy, F. Calle, and F. Omnes, Appl. Phys. Lett. **81**, 1902 (2002).
18. J. J. Yu and I. W. Boyd, Diamond Relat. Mater. **16**, 494 (2007).
19. O. M. Nayfeh, S. Rao, A. Smith, J. Therrien, and M. H. Nayfeh, IEEE Photon. Technol. Lett. **16**, 1927 (2004).
20. S. Butun, T. Tut, B. Butun, M. Gokkavas, H. Yu, and E. Ozbay, Appl. Phys. Lett. **88**, 123503 (2006).
21. G. Ariyawansa, M. B. M. Rinzan, M. Alevli, M. Strassburg, N. Dietz, A. G. U. Perera, S. G. Matsik, A. Asghar, I. T. Ferguson, H. Luo, A. Bezinger, and H. C. Liu, Appl. Phys. Lett. **89**, 091113 (2006).